Research Article

Basic Physics Model for PdH Thermodynamics

Peter Orondo and Peter L. Hagelstein*

Research Laboratory of Electronics, Massachusetts Institute of Technology, Cambridge, MA 02139, USA

Abstract

We made use of the very powerful modern density functional code Quantum Espresso for an ab initio calculation of the thermodynamics of PdH. There is an energy offset of about 100 meV in the calculation as compared to experiment. We developed an empirical correction to the theoretical energies which allowed us to fit the experimental results for excess enthalpy and excess entropy with some success. We also explored a new model that posits a weak binding between absorbed hydrogen atoms in PdH, and is able to provide a better fit to the experimental results. The model provides a simple physical explanation of observed phase diagram, and also of the observed dependence of the thermodynamic variables (excess enthalpy and excess entropy) on loading.
© 2014 ISCMNS. All rights reserved. ISSN 2227-3123

Keywords: Density functional calculation, Phase diagram, Quantum espresso, Thermodynamics

1. Introduction

Palladium hydride is one of the most studied and best understood of the metal hydrides. However, a complete picture of the physics and thermodynamics of absorbed hydrogen still eludes us.

Early work on the theory of absorbed interstitial hydrogen was done by Fowler [1] and Lacher [2]. They attempted to model the properties of absorbed hydrogen using a statistical interpretation. From this point of view, a distribution of the gas and hydrogen in metal phases may be derived from the partition function after assuming that the lattice contains potential energy holes into which the hydrogen is absorbed [2]. A challenge, however, arises because the energy of the absorbed hydrogen has to be known a high degree of accuracy if such a scheme is to give good results.

Earlier workers have tackled the problem with varying degrees of success. Christensen employed an effective medium-type model within the same partition function formalism as Lacher's [3] while Salomons has employed molecular dynamics [4]. There are also Monte Carlo models, for example [5]. In this work we make use of an ab initio calculation based on modern density functional methods as implemented in Quantum Espresso.

2. Basic Model Formulation

In this work, we employ the basic Lacher model to describe the entire problem, so we write
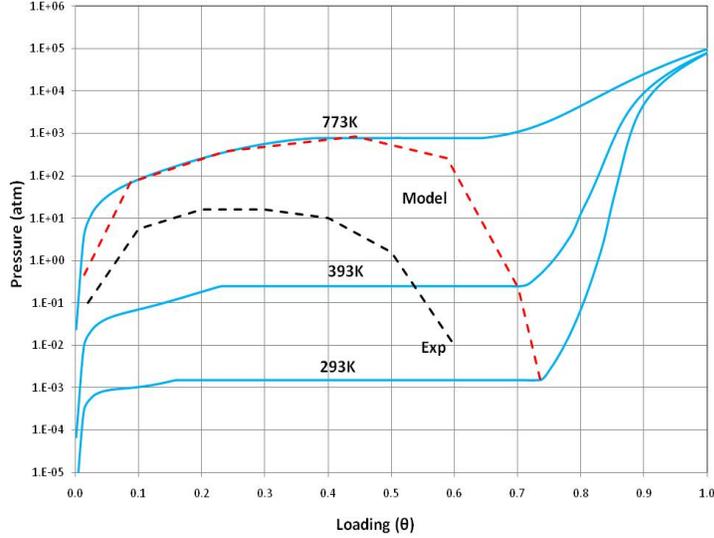
---

*E-mail: plh@mit.edu

Figure 1. Pressure-composition-temperature isotherms; phase boundary from experiment (*black*); model isotherms (*blue*); model phase boundary (*red*).

$$Z_H(\tau, \mu) = \sum_{n_o} \sum_{n_t} \sum_{ASN} e^{\frac{(n_o + n_t)\mu - \epsilon_h}{\tau}} z^{(n_o + n_t)}. \tag{1}$$

In Eq. (1), $Z_H(\tau, \mu)$ is the grand partition function of the full PdH system; $n = n_o + n_t$ is the number of occupied sites, of which there are two types, shown in subscripts (octahedral and tetrahedral); τ is the normalized temperature $\kappa_B T$; μ is the chemical potential of absorbed proton; Z is the partition function of an absorbed proton; $\epsilon_h(n)$ is the total interaction energy of the configuration containing n absorbed protons; and "ASN" signifies all configurations containing $n_o + n_t$ absorbed protons.

From the grand partition function, the system is fully characterized (if we could determine the interaction energy accurately). Thus, the chemical potential of the interstitial proton is, for example, for the occupied octahedral sites,

$$\mu_o(\tau, n_o, n_t) = -\tau \frac{\partial \ln Z_H(\tau, n_o, n_t)}{\partial n_o}, \tag{2}$$

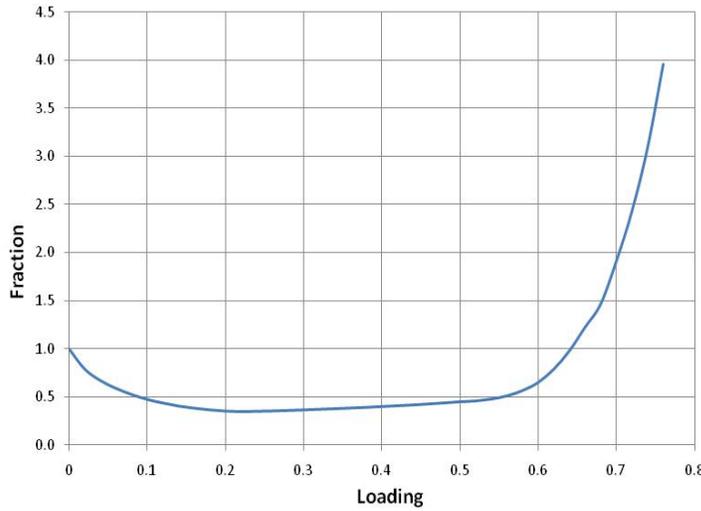which must equal that of the tetrahedral species. The result is, after using the Stirling approximation:

Figure 2. Incremental number of accessible microstates for data from [11].

$$\mu_H(\theta) = -\tau \ln z + \tau \ln \frac{\theta}{1-\theta} + \theta \frac{\partial}{\partial \theta} \epsilon_h(\theta) + \epsilon_h(\theta), \tag{3}$$

where $\theta = n/N$ is fractional occupation or loading, and N is the total number of available interstitial sites.

Matching the chemical potential at the gas–solid boundary then yields an analytical expression for the pressure–composition–temperature isotherm. The gas phase chemical potential is well known, for example [6]:

$$\mu_{H_2} = -\tau \ln \left[\left(\frac{2\pi m\tau}{h^2} \right)^{3/2} \frac{\tau}{P} \right] - \tau \ln \frac{e^{\frac{\epsilon_{0v}}{2\tau}}}{1 - e^{\frac{\epsilon_{0v}}{\tau}}} - \tau \ln \left(\frac{8\pi^2 I \tau}{\sigma h^2} \right) - \epsilon_D. \tag{4}$$

In Eq. (4), the right-hand side terms are, respectively, the translational, vibrational, rotational and dissociative contributions to chemical potential of hydrogen gas. At high pressure, we must use fugacity instead of pressure in Eq. (4).

3. Density Functional Theory: State Energies

For the dissolved hydrogen, we calculate the state energies by developing approximate solutions to the many-body time-independent Schrodinger equation:
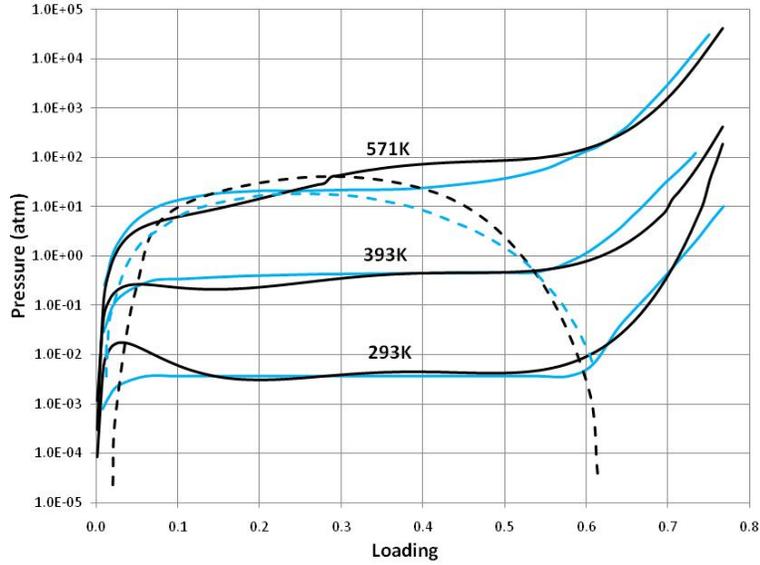
Figure 3. P–C–T isotherms; model (*black*); experiment (*blue*).

$$\hat{H}\psi(r_i) = E_i\psi(r_i), \tag{5}$$

where

$$\hat{H} = -\sum_i \frac{\hbar^2 \nabla_i^2}{2m_e} - \sum_{i,I} \frac{Z_I e^2}{|\mathbf{r}_i - \mathbf{R}_I|} + \sum_{i \neq j} \frac{e^2}{|\mathbf{r}_i - \mathbf{r}_j|} - \sum_I \frac{\hbar^2 \nabla_I^2}{2M_I} + \frac{1}{2} \sum_{I,J} \frac{Z_I Z_J e^2}{|\mathbf{R}_J - \mathbf{R}_I|}. \tag{6}$$

The Hamiltonian is made up of kinetic and Coulomb potential energy contributions in a nonrelativistic approximation.

Given the substantial progress made in recent years in density functional codes, we decided to make use of Quantum Espresso and work with density functional theory (DFT) to obtain approximate solutions to Eq. (5). Additionally, we need to give a meaning to the interaction energy term, $\epsilon_h(n)$. For that, we make a simple definition that corresponds to the energy change when one proton is absorbed, referenced to the gas energy in vacuum, ϵ_{2H}^{Vac}:

$$\epsilon_h(n) = \epsilon_{(n+1)H}^{Pd} - \left(\epsilon_{nH}^{Pd} + \frac{1}{2}\epsilon_{2H}^{Vac} \right). \tag{7}$$
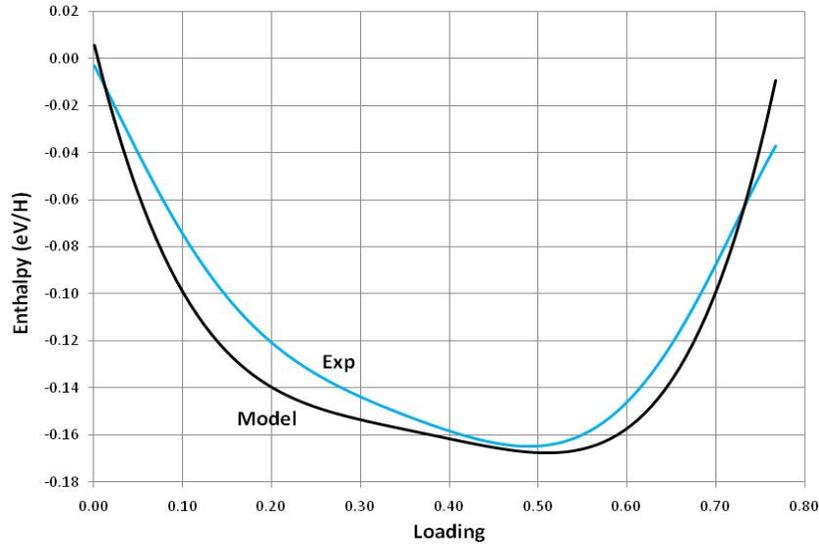
Figure 4.   Model excess enthalpy at 571 K; experimental data is from [11].

From the solution for this energy we obtain the pressure–composition–temperature isotherm of Fig. 1 from Eqs. (3) and (4). We find that the DFT results are correct qualitatively; but corrections will be required in order to obtain agreement with experimental results for the chemical potential.

4. Corrected Energy

We would like to take this basic DFT result above and correct it in a manner consistent with the expected relevant physics. We assume that the biggest errors are associated with the DFT calculation of the state energies. Apart from the constant offset in calculated DFT energies which are intrinsic in the model (see e.g. [7]), there will be corrections from the interaction of H with the Pd lattice. These errors are plausibly expected to be linear in loading. We should also expect that DFT will not correctly predict elasticity that is inevitable when the lattice expands with loading. We expect these errors to be quadratic. Lastly, DFT will not capture any temperature dependence of the energy; we recall that band energies in semiconductors are often linear in temperature (see [8] e.g.), and there is no reason to expect the energies in PdH to behave differently.

This discussion motivates us to consider a corrected energy model given of the form [9]

$$\epsilon_h(\theta, T) \rightarrow \epsilon_h(\theta) + \left[\epsilon_\delta^0 + \epsilon_\delta^0(T - T_c)\right] + \left[\epsilon_\delta^1 + \epsilon_\delta^1(T - T_c)\right]\theta + \left[\epsilon_\delta^2 + \epsilon_\delta^2(T - T_c)\right]\theta^2 + O(\theta^3), \qquad (8)$$
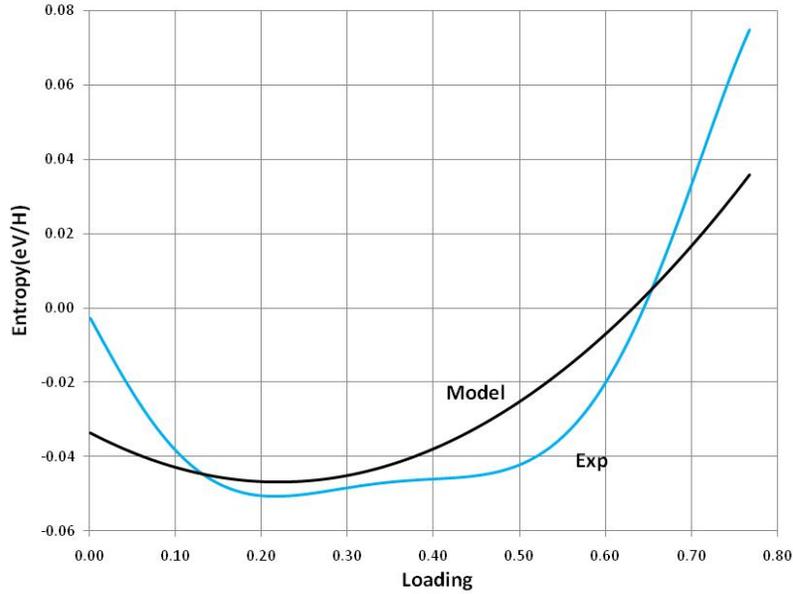
Figure 5.   Excess enthalpy at 571 K; model (*black*) ; experiment [11] (*blue*).

where, $\epsilon_\delta^0, \epsilon_\delta^1, \epsilon_\delta^2, \epsilon_\delta^0, \epsilon_\delta^1, \epsilon_\delta^2$ are fitting parameters that are determined based on a global fit to experimental P–C–T, and enthalpy and entropy data and T_c is set to the critical temperature for convenience.

5. Excess Enthalpy, Excess Entropy

In a straightforward manner, we can calculate excess entropy and excess enthalpy [9] from the pressure derived analytically from Eqs. (3) and (4). The results are

$$H = -T^2 \left(\frac{\partial (\frac{G}{T})}{\partial T} \right)_{P,n}.$$ (9)

In Eq. (9), H is enthalpy and G is the Gibbs energy. From this, we can derive excess $\overline{H}_H^E$ enthalpy, via [10]

$$\Delta \overline{G}_H = \overline{G}_H^{\text{Ideal}} + \Delta \overline{G}_H^{\text{Excess}}$$ (10)
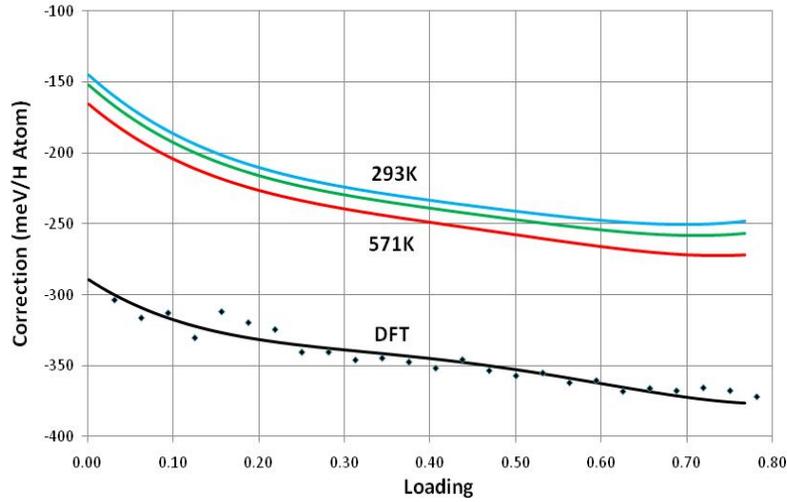
and

Figure 6. DFT interaction energy (*black*); corrected interaction energy (in color, showing temperature dependence).

$$\overline{G}_H^{Ideal} = RT \ln \frac{\theta}{1-\theta} \tag{11}$$

as

$$\overline{H}_H^E = \Delta \overline{H}_H^E - \Delta \overline{H}_H^0, \tag{12}$$

where $\Delta \overline{H}_H^0$ is the enthalpy at zero loading [11] and we have converted Eq. (9) to the usual molar format.

Excess entropy may be derived similarly [9]. Thus,

$$-S = \left(\frac{\partial G}{\partial T} \right)_{P,n} \tag{13}$$

and, similar to Eq. (12)

$$\overline{S}_H^E = \Delta \overline{S}_H^E - \Delta \overline{S}_H^o. \tag{14}$$
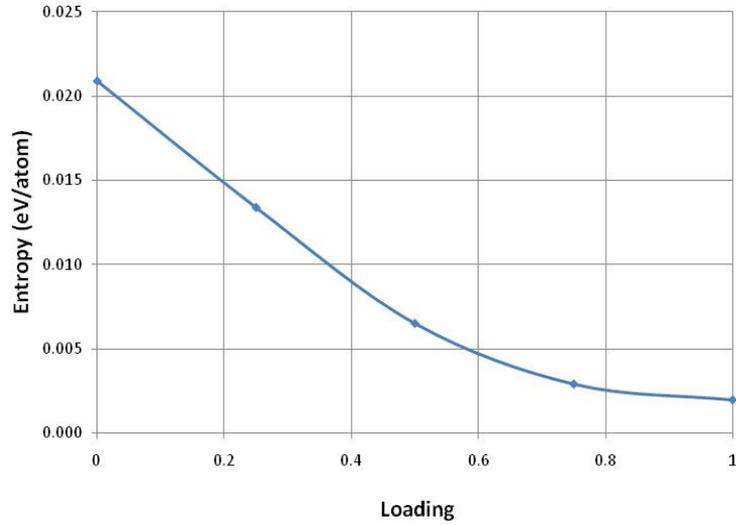
Figure 7.   Model electronic entropy at 571 K.

Now, we interpret the excess entropy as telling us something about the incremental number of accessible proton microstates in metal hydride [9]. To see this, we apply the fundamental definition of entropy to write:

$$\overline{S}_H^E = \kappa_{\mathrm{B}} \ln \Omega^E, \tag{15}$$

where Ω^E may now be thought of as the incremental number of accessible microstates from the gas phase (initial) to the absorbed state (final), i.e.,

$$\Omega^E = \frac{\Omega^{\mathrm{final}}}{\Omega_{\mathrm{initial}}}. \tag{16}$$

For the experimental data we used in this work [11], we can depict Eq. (16) in Fig. 2. From this point of view, we see that the experimental excess entropy is consistent with a reduction of about half the number of accessible microstates in the miscibility gap. As the loading increases above the miscibility gap, the number of accessible microstates also increases.
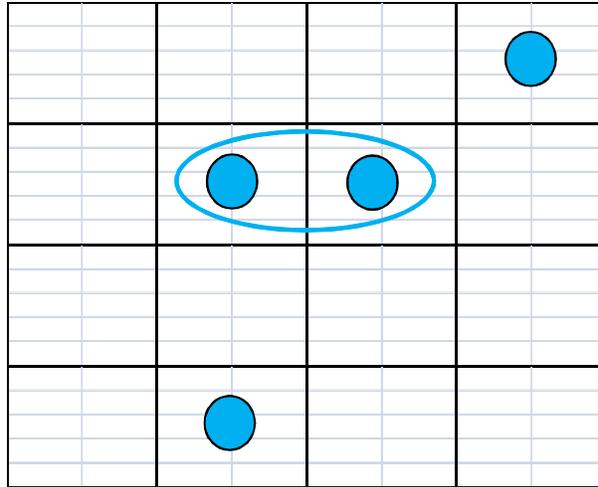
Figure 8. Hydrogen quasi-molecule based on a proposed attractive interaction between neighboring interstitial hydrogen in PdH at low H concentration.

6. Results

Applying these corrections to the basic model, Eqs. (1), (7) and (8), we get a marked improved in our match to experiment; Fig. 3 shows the improved PCT isotherms. From Eqs. (12) and (15), we may derive excess enthalpy and entropy analytically; the results are shown in Fig. 4.

The results for excess entropy and enthalpy compare well with experiment. The corrected interaction energy in this model is shown in the colored curves of Fig. 6; we see that the correction is roughly 100 meV, with a weak dependence on the temperature. DFT results for specific configurations are shown as dots, with the average shown as a black line.

A spread in the energies associated with the different configurations would by itself produce a temperature dependence in the weighted average that would produce corrections that would increase with temperature. The corrections obtained by matching this model to data decrease in temperature. In the Appendix we discuss a different model that assumes possible pairing between interstitial hydrogen; in that model the corrected energy increases with temperature.

7. Electronic Contributions to Entropy

Kuji [11] has proposed that electronic contributions to entropy might dominate at high loading. We have attempted to evaluate this position in a couple of ways. First, we modeled the electronic contributions to entropy as a correction to the proton chemical potential. Thus, we formulated the problem using the partition function
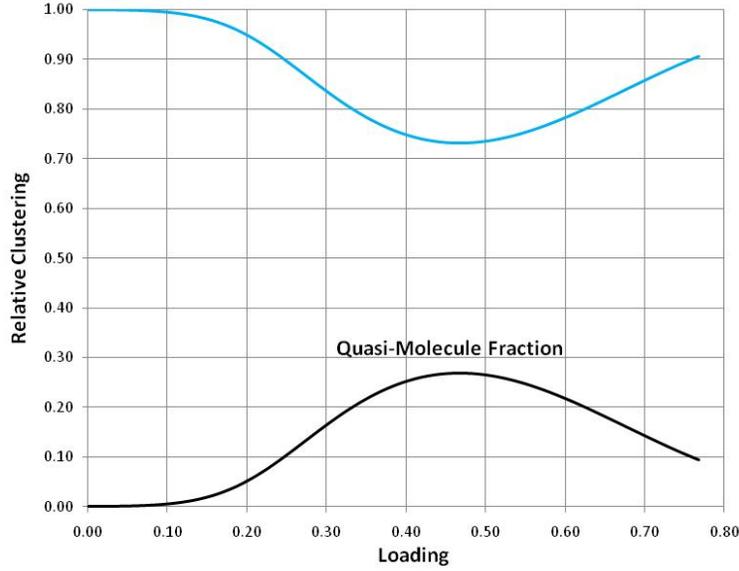
Figure 9. Quasi-molecule fraction from optimization of the model.

$$Z_H(\tau, \mu) = \sum_k \sum_\sigma \left(\sum_{n_{nc}=0}^{N_o} \sum_{k=o}^{\frac{N_o-n_{nc}}{\alpha+\gamma}} \sum_{n_T=0}^{N_t} \sum_{ASN} e^{\frac{(n_{nc}+n_t+k\gamma)\mu - \epsilon_h(n)}{\kappa_B T}} z_o^{n_{nc}} z_t^{n_t} z_c^{k\gamma} z_{e,t}^{n_t} z_{e,c}^{k\gamma} \right)$$
$$g_k^\sigma e^{\frac{\epsilon_\sigma(n,\kappa) - \mu_F(n,\tau)}{\kappa_B T}}. \tag{17}$$

In this formulation, g_k^σ is the degeneracy of the kth electronic band with spin α. After evaluating the electronic contribution obtained from this model, we found that it was negligible [9].

A second approach is to consider the electronic and proton contributions as approximately independent and write [13]

$$\overline{\mu}_H^E(\theta, T) = \overline{\mu}_{H^+}^E(\theta, T) + \overline{\mu}_F^E(\theta, T), \tag{18}$$

where the proton contribution, $\overline{\mu}_F^E(\theta, T)$, was previously modeled above. For the electronic portion, we use the basic theoretical result [14], and calculate it from first principles using DFT [9]:
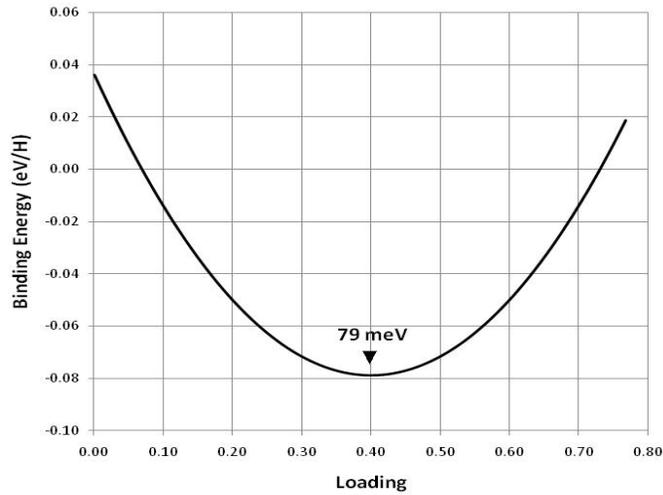
Figure 10.   Quasi-molecule binding energy at 571 K.

$$S_E(x) = -\int g(\epsilon)d\epsilon \left[f_{\mathrm{FD}} \ln f_{\mathrm{FD}} + (1 - f_{\mathrm{FD}}) \ln(1 - f_{\mathrm{FD}}) \right], \tag{19}$$

where f_{FD} is the Fermi Dirac function, $g(\epsilon)$ is the density of states, and

$$x(\tau) = \frac{\mu - \varepsilon_l(n)}{\tau}. \tag{20}$$

The results are shown in Fig. 7; this is inconsistent with Kuji [11], but consistent with Wallace [14].

8. Discussion

In the work outlined here, we developed a physics-based model that describes the hydrogen absorption into palladium lattice. Using a statistical mechanics and the grand partition function formalism, we are able to obtain a theoretical expression for basic properties of hydrogen absorption in equilibrium.

In recent years density functional theory has become much more widely used for applied problems in materials science in general, and for hydrogen in metals in particular. We have taken advantage of the availability of Quantum Espresso, and of the increasing power of modern computers, to use DFT to study hydrogen absorption in palladium.
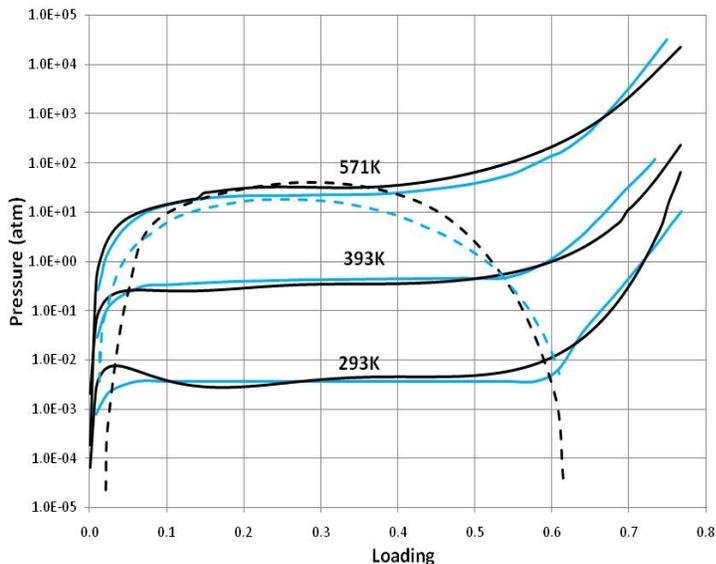
Figure 11.   P–C–T Isotherms; model (*black*); experiment [12] (*blue*).

We know that modern DFT calculations are very good; however, the independent particle approximation has limitations as an approximation, and we would not expect the DFT energies to match experimental ones. Since PdH is one of the best studied metal hydrides, we have thermodynamic data that allows us to compare the DFT results with experiment (since there are no experimental results for the interaction energy). Based on the initial comparison illustrated in Fig. 1, we know that there are errors in the DFT results, and we were hoping to quantify them. As the research progressed, it became apparent that we could do more than just quantify DFT errors, we found that we could correct them in a meaningful way, leading to a corrected energy that seems to give results globally that are close to experiment. This is interesting, and results in a new physics-based model that can be used in future work.

This kind of model is in some sense the simplest possible that might be relevant to PdH; hydrogen occupation of interstitial sites is essentially random with a thermal weighting associated with the average energy. In this model the occurrence of the miscibility gap is due to the dependence of the underlying chemical potential as a function of loading, following the argument of Lacher. However, we know that segregation occurs in NiH in the miscibility gap, which indicates that hydrogen–hydrogen attraction occurs. Since NiH and PdH are closely related, it would be natural to consider the possibility of a hydrogen–hydrogen attraction in PdH. For example, quasi-molecule formation due to singlet electronic state occupation which is not included in the DFT calculation could provide a physical basis for such an effect. If we interpret the excess entropy in the miscibility gap in terms of a reduction in the number of accessible microstates as illustrated in Fig. 2, we might conclude than ordering of some kind occurs; a model with pairing would
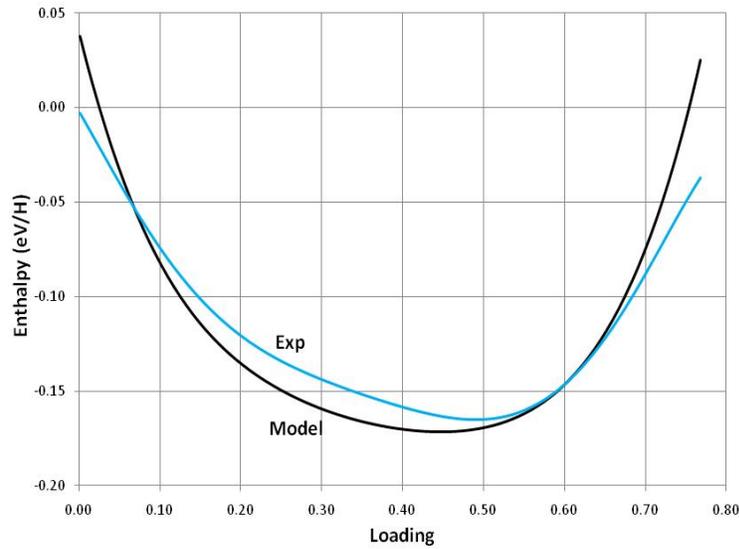
Figure 12.   Excess enthalpy at 571 K; model (*black*); experiment [11] (*blue*).

be expected to show such a reduction in excess entropy naturally. In the Appendix we discuss a model for PdH which works in this way.

Appendix A.

As part of our research on PdH work, we investigated a model whereby a weak binding between neighboring absorbed protons [9] through the sharing of a localized electron pair to form a quasi-molecule as shown in Fig. 8. Such a binding is might occur due to electronic occupation of a quasi-molecule singlet state, or perhaps due to simple polarization effects; occupation of quasi-molecule states constitutes an ordering that is consistent with the excess entropy in the miscibility gap. We assume that the binding energy has a dependence on loading and temperature similar to the interaction energy discussed in the main text; the form of the binding is taken to be

$$E_B^c(\theta) \rightarrow \epsilon_c^c + \delta_c^c(T - T_c) + \left[\epsilon_c^1 + \delta_c^1(T - T_c)\right]\theta + \left[\epsilon_c^2 + \delta_c^2(T - T_c)\right]\theta^2 + O(\theta^3). \qquad (A.1)$$

In Eq. (A.1), ϵ_c^0, ϵ_c^1, ϵ_c^2, δ_c^0, δ_c^1, and δ_c^2 are fitting parameters that are determined based on a global fit to experimental P–C–T, and enthalpy and entropy data.
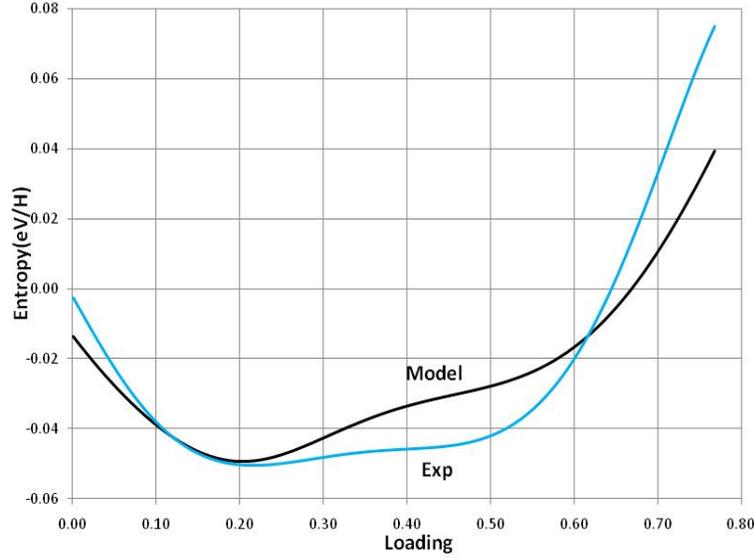
Figure 13. Excess entropy at 571 K; model (*black*); experiment [11] (*blue*).

If one postulates the existence of a quasi-molecule at low concentration, then there are issues about what occurs at high concentration (where additional hydrogen occupation of nearby states occurs). We have investigated two different models, the most interesting of which is one where we assume that the quasi-molecule is destroyed when additional protons are present in adjacent sites. The resulting exclusion model is then [9]

$$Z_H(\tau\mu) = \sum_{n_{nc}=0}^{N_o} \sum_{k=0}^{\frac{N_o-n_{nc}}{\alpha+\gamma}} \sum_{n_t=0}^{N_t} \sum_{ASN} e^{\frac{(n_{nc}+n_t+k\gamma)\mu-\epsilon_h}{\tau}} z_o^{n_{nc}} z_t^{n_t} z_c^{k\gamma} z_{e,o}^{n_{nc}} z_{e,t}^{n_t} z_{e,c}^{k\gamma}, \tag{A.2}$$

where γ is a clustering factor, α is a nearest-neighbor exclusion factor, and we have added electronic contribution terms to the partition function – for example $z_{e,o}^{n_{nc}}$ is the electronic contribution to the partition function of an electron 'associated' with a non-clustered proton [9].

The model we posit in Eq. (A.2) predicts a quasi-molecule population given by the following isotherm [9].

$$\varphi^{\frac{1}{\gamma}} \frac{\theta_c^{\frac{1}{\gamma}} (1-\theta_{nc})^{\frac{\gamma\varphi-1}{\gamma\varphi}}}{\theta_{nc}(1-\theta_{nc}-\varphi\theta_c)^{\frac{\varphi-1}{\gamma\varphi}}} = \frac{1}{2}\left(1-e^{-\frac{\epsilon_{ov}}{k_B T}}\right)^3 e^{-\frac{E_B^c(n)}{\kappa_B T}}, \tag{A.3}$$
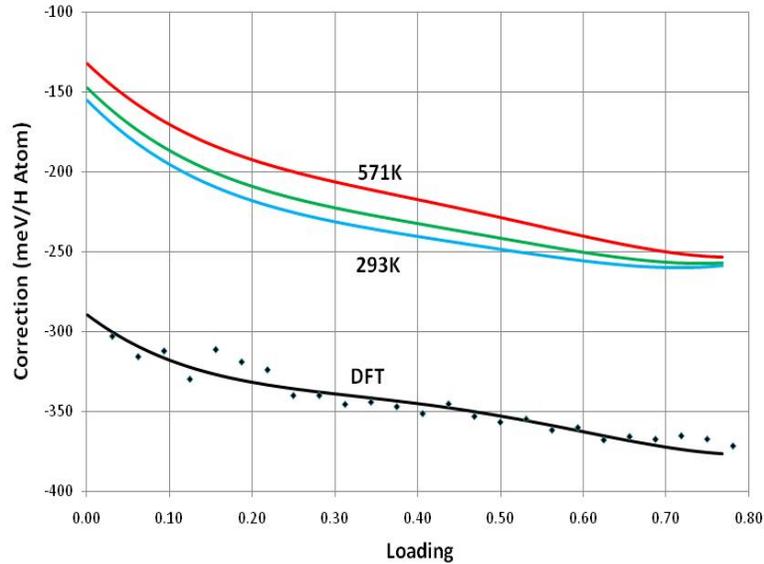
Figure 14. Interaction energy corrections for the pairing model.

where

$$\varphi = \frac{\alpha + \gamma}{\gamma}. \tag{A.4}$$

Equation (A.3) predicts significant fractional quasi-molecule population in the miscibility gap, after optimization of the model against experimental P–C–T data, excess entropy, and excess enthalpy. Results at 571 K are shown in Fig. 9.

The model predicts a quasi-molecule population that peaks around the middle of the miscibility gap. It may be that with a more sophisticated version of this kind of model that we might think of the two phases in the miscibility gap as random and ordered, where the ordering is due to quasi-molecule formation. The binding energy for the quasi-molecule is shown in Fig. 10. From this result, we see that the model binding energy is relatively weak (79 meV), as expected. The binding profile has a minimum near the middle of the miscibility gap. We also show the results based on a global, simultaneous fit to P–C–T isotherms at three temperatures (Fig. 11), and excess enthalpy (Fig. 12) and excess entropy (Fig. 13).

We can obtain somewhat better agreement between model and data with this more complicated model, although this does not adequately bring out how the model accomplishes this. In the simpler model described in the main text, the excess entropy is matched by decreasing the interaction energy with temperature; in this model the excess entropy

is matched in the miscibility gap by reducing the number of accessible microstates, and the interaction energy increases with temperature (Fig. 14).

Note that the apparent divergence between model and experiment in the high loading regime in the plots in this paper is due in part to the weights used in the least squares fits. These results are in a sense preliminary due to the way the fits were obtained.

References

[1]   R. Fowler, *Proc. Camb. Phil. Soc.* **32** ((1936) 144.
[2]   J. Lacher, *Proc. R. Soc. Lond. A* **161** (1937) 525.
[3]   O. Christensen, P. Stoltze and W. Jacobsen, *Norskov J. Phys. Rev. B* **41** (1990) 12413.
[4]   E. Salomons, *J. Phys: Cond. Mat.* **2** (1990) 845.
[5]   R. Wolf et al., *Phys. Rev. B* **48** (1993) 12415.
[6]   Silbey, Alberty and Bawendi, *Physical Chemistry* (Wiley, New York).
[7]   R. Martin, *Electronic Structure* (Cambridge University Press, Cambridge, 2004).
[8]   F. Stern and S. Sarma, *Phys. Rev. B* (1984) 840.
[9]   P. Orondo, MIT Ph.D. Thesis, 2012.
[10]   G. Boureau, O. Kleppa and P. Dantzer, *J. Chem. Phys.* **64** (1976) 5247.
[11]   T. Kuji, W. Oates, B. Bowerman and T. Flanagan, *J. Phys. F: Met. Phys.* **13** (1983) 1785.
[12]   E. Wicke and F. Brodowsky (*Hydrogen in Metals II.*, 1978).
[13]   W. Oates and A. Stoneham, *J. Phys. F.: Met. Phys.* **13** (1983) 2427.
[14]   D. Wallace, *Phys. Rev. B* 46 (1992) 5242.